Sensors **2011**, *11*, 886-904; doi:10.3390/s110100886

OPEN ACCESS

sensors

ISSN 1424-8220

www.mdpi.com/journal/sensors

Supporting Information

Porphyrin-Embedded Silicate Materials for Detection of Hydrocarbon Solvents

Brandy J. Johnson *, Nicole E. Anderson, Paul T. Charles, Anthony P. Malanoski, Brian J. Melde, Mansoor Nasir and Jeffrey R. Deschamps

Center for Bio/Molecular Science and Engineering, Naval Research Laboratory, Washington, D.C. 20375, USA; E-Mails: nanders2@umd.edu (N.E.A); paul.charles@nrl.navy.mil (P.T.C.); anthony.malanoski@nrl.navy.mil (A.P.M.); brian.melde@nrl.navy.mil (B.J.M.); mansoor.nasir@nrl.navy.mil (M.N.); jeff.deschamps@nrl.navy.mil (J.R.D.)

* Author to whom correspondence should be addressed; E-Mail: brandy.white@nrl.navy.mil; Tel.: +1-202-404-6100; Fax: +1-202-767-9598.

Received: 1 December 2010; in revised form: 5 January 2011 / Accepted: 13 January 2011 / Published: 14 January 2011

The supplementary data supplied here provides complete results of structural characterization and image analysis for exposure of the various materials to hexane, benzene, and toluene. A list of the metal salts used to generate metalloporphyrin variants is provided. Additional absorbance and fluorescence results and reflectance spectra are also included.

Table S1. Metal salts used in the preparation of metalloporphyrin variants.

magnesium chloride	copper (II) chloride	vanadium (III) bromide
yttrium (III) chloride	zinc chloride	ruthenium (III) chloride
titanium (II) chloride	silver chloride	praseodynium (III) chloride
manganese (II) chloride	cadmium chloride	cerium (III) chloride
iron (III) chloride	tin (II) chloride	europium (II) chloride
cobalt (II) chloride	platinum (IV) chloride	osmium (III) chloride
nickle (II) chloride	gold (III) chloride	

Table S2. Results of rapid screening for interaction of porphyrins with targets in solution. For C_1TPP and C_4TPP, results for the four selected candidates and the next four highest performers are provided. For C_1S_3TPP, results for the top six performers are provided.

Porphyrin	Target	Δ λ	Δ I	Porphyrin	Target	Δ λ	Δ I
C_1TPP	Benzene	8	0.062	C_4TPP	Benzene	9	0.078
	Toluene	9	0.134		Toluene	11	0.215
	Hexane	--	--		Hexane	8	0.039
FeC_1TPP	Benzene	8	0.502	FeC_4TPP	Benzene	--	0.038
	Toluene	--	--		Toluene	--	0.094
	Hexane	8	0.462		Hexane	10	0.096
CuC_1TPP	Benzene	10	0.145	MnC_4TPP	Benzene	--	0.188
	Toluene	12	0.222		Toluene	--	0.127
	Hexane	--	--		Hexane	--	0.083
MnC_1TPP	Benzene	10	0.139	ZnC_4TPP	Benzene	9	0.073
	Toluene	8	0.199		Toluene	8	0.054
	Hexane	7	0.030		Hexane	--	0.095
ZnC_1TPP	Benzene	6	0.083	CoC_4TPP	Benzene	9	0.042
	Toluene	7	0.053		Toluene	8	0.043
	Hexane	4	0.016		Hexane	10	0.018
CoC_1TPP	Benzene	8	0.097	CuC_4TPP	Benzene	9	0.076
	Toluene	9	0.033		Toluene	7	0.062
	Hexane	8	0.016		Hexane	7	0.014
MgC_1TPP	Benzene	9	0.098	MgC_4TPP	Benzene	8	0.058
	Toluene	8	0.084		Toluene	8	0.039
	Hexane	8	0.023		Hexane	--	0.043
NiC_1TPP	Benzene	9	0.093	NiC_4TPP	Benzene	10	0.047
	Toluene	10	0.049		Toluene	9	0.084
	Hexane	12	0.056		Hexane	--	0.026
C_1S_3TPP	Benzene	6	0.015	MnC_1S_3TPP	Benzene	9	0.012
	Toluene	6	0.032		Toluene	6	0.009
	Hexane	6	0.01		Hexane	8	0.033
FeC_1S_3TPP	Benzene	--	0.018	CuC_1S_3TPP	Benzene	--	0.023
	Toluene	--	0.011		Toluene	--	0.024
	Hexane	--	--		Hexane	6	0.02
NiC_1S_3TPP	Benzene	--	0.016	ZnC_1S_3TPP	Benzene	8	0.029
	Toluene	--	0.014		Toluene	6	0.008
	Hexane	--	--		Hexane	--	0.004

Table S3. Interaction of candidate porphyrins with targets in solution.

		Rapid Screening		**Binding Isotherm**		
Porphyrin	**Target**	**Δ λ**	**Δ I**	**K_{11} (1/M)**	**$\Delta\varepsilon_{11}$ Peak (A/M)**	**$\Delta\varepsilon_{11}$ Trough (A/M)**
C_1TPP	Benzene	8	0.062	2.1	1,250	2,580
	Toluene	9	0.134	6.3	522	586
	Hexane	--	--	--	--	--
FeC_1TPP	Benzene	8	0.502	1.0	3,500	2,540
	Toluene	--	--	--	--	--
	Hexane	8	0.462	2.5	5,240	1,340
CuC_1TPP	Benzene	10	0.145	150	20,860	398
	Toluene	12	0.222	9.8	594	1,440
	Hexane	--	--	--	--	--
MnC_1TPP	Benzene	10	0.139	10	19,030	18,680
	Toluene	8	0.199	5.1	178,000	12,180
	Hexane	7	0.030	120	3,210	2,650
C_4TPP	Benzene	9	0.078	2.0	65,910	42,770
	Toluene	11	0.215	0.9	76,130	43,500
	Hexane	8	0.039	1.7	107,600	32,550
FeC_4TPP	Benzene	--	0.038	17	--	53,420
	Toluene	--	0.094	26	--	25,380
	Hexane	10	0.096	13	--	30,450
MnC_4TPP	Benzene	--	0.188	1.0	--	132,400
	Toluene	--	0.127	7.1	--	38,060
	Hexane	--	0.083	7.3	--	22,720
ZnC_4TPP	Benzene	9	0.073	0.7	60,900	43,500
	Toluene	8	0.054	5.5	27,680	12,690
	Hexane	--	0.095	8.0	--	19,030

Figure S1. Structural characterization. Panel A, nitrogen sorption isotherms (DEB shifted by +240 and TM1 shifted by +250). Panel B, pore size distributions. Panel C, XRD spectra. (DEB–blue, TM1–red, Ph1–black, PhE1–green).

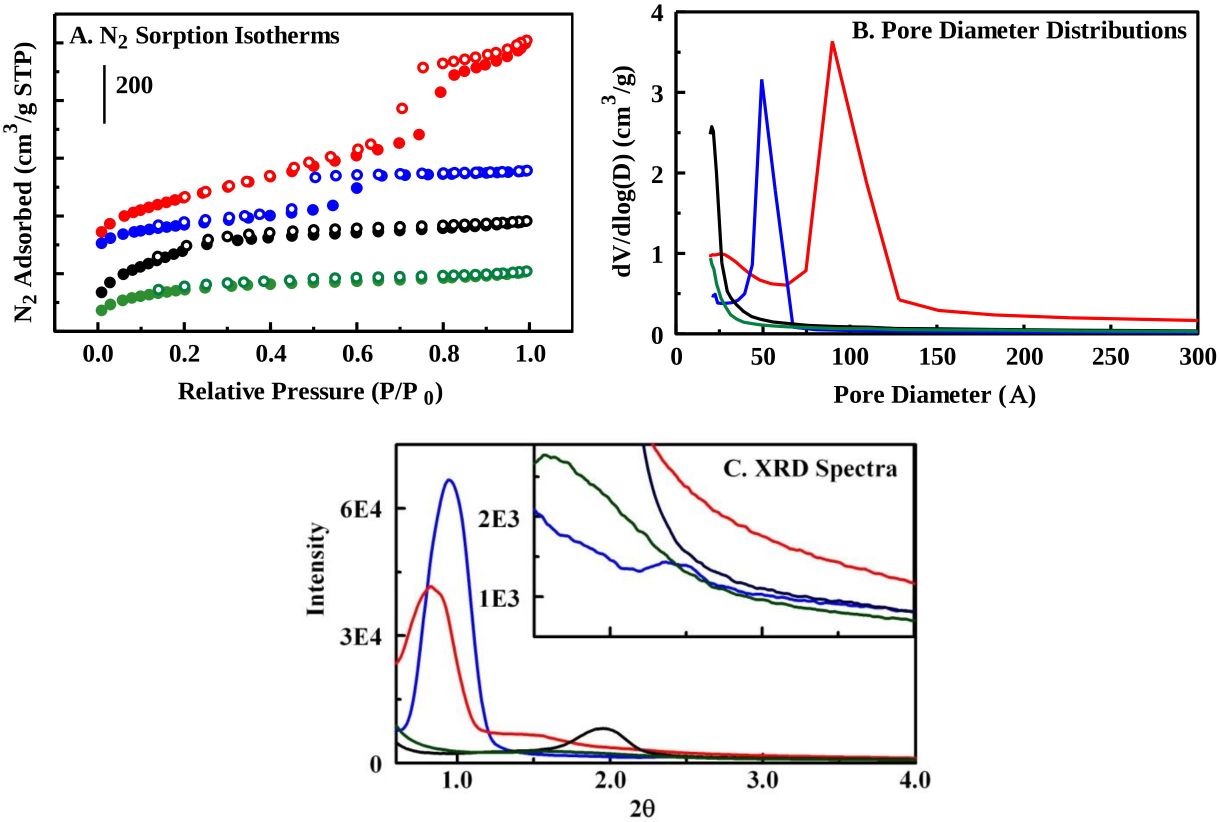

Figure S2. BTEX binding capacity. Shown here is the amount of each BTEX component bound by the sorbents (200 mg). BTEX (209 mg—equal volumes benzene, toluene, ethylbenzene, and xylene) binding was evaluated in vapor phase.

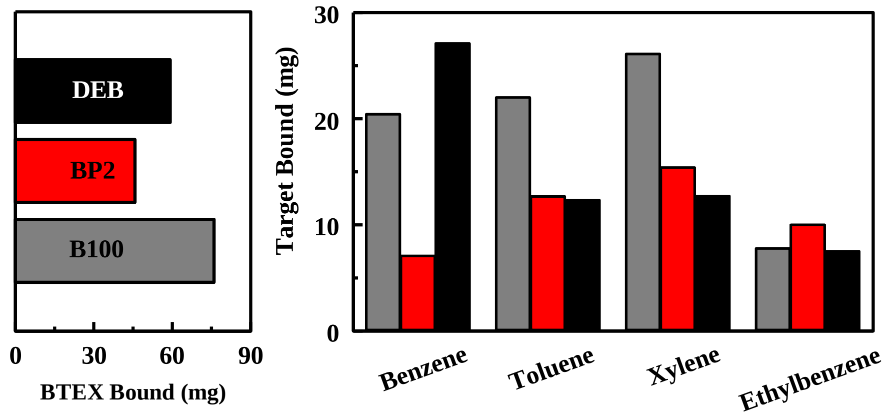

Figure S3. Dependence on concentration of the interaction between metalloporphyrins and targets in solution (benzene–red, toluene–green, hexane–blue).

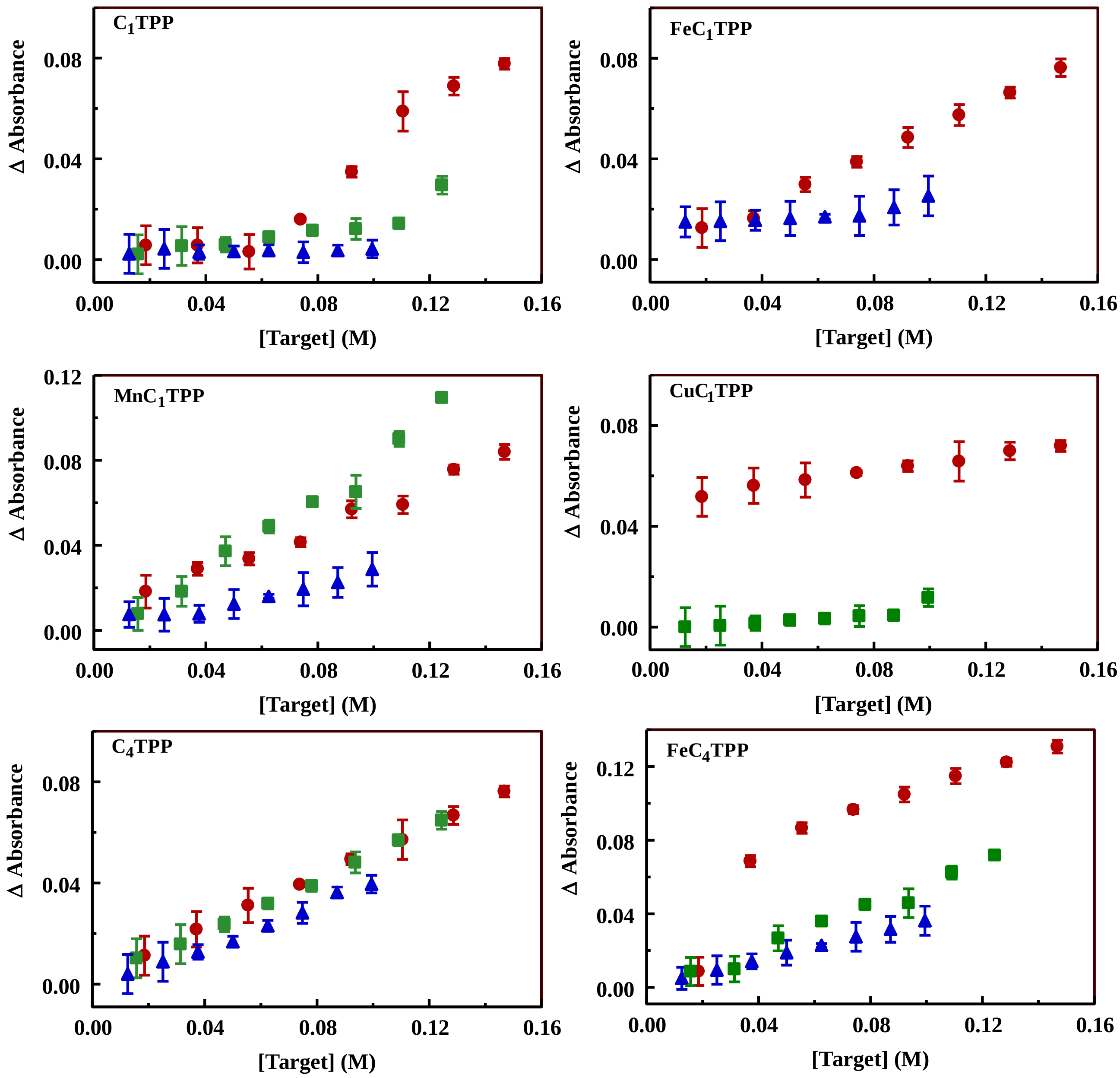

Figure S4. Interaction of FeC_1TPP-embedded B100 with targets. Shown here are the changes in fluorescence characteristics and the dependence of RGB image color values on target concentration for the interaction of targets with FeC_1TPP-embedded B100. Changes in fluorescence intensity versus concentration are based on peak/trough differences generated by peak fitting the excitation difference spectra.

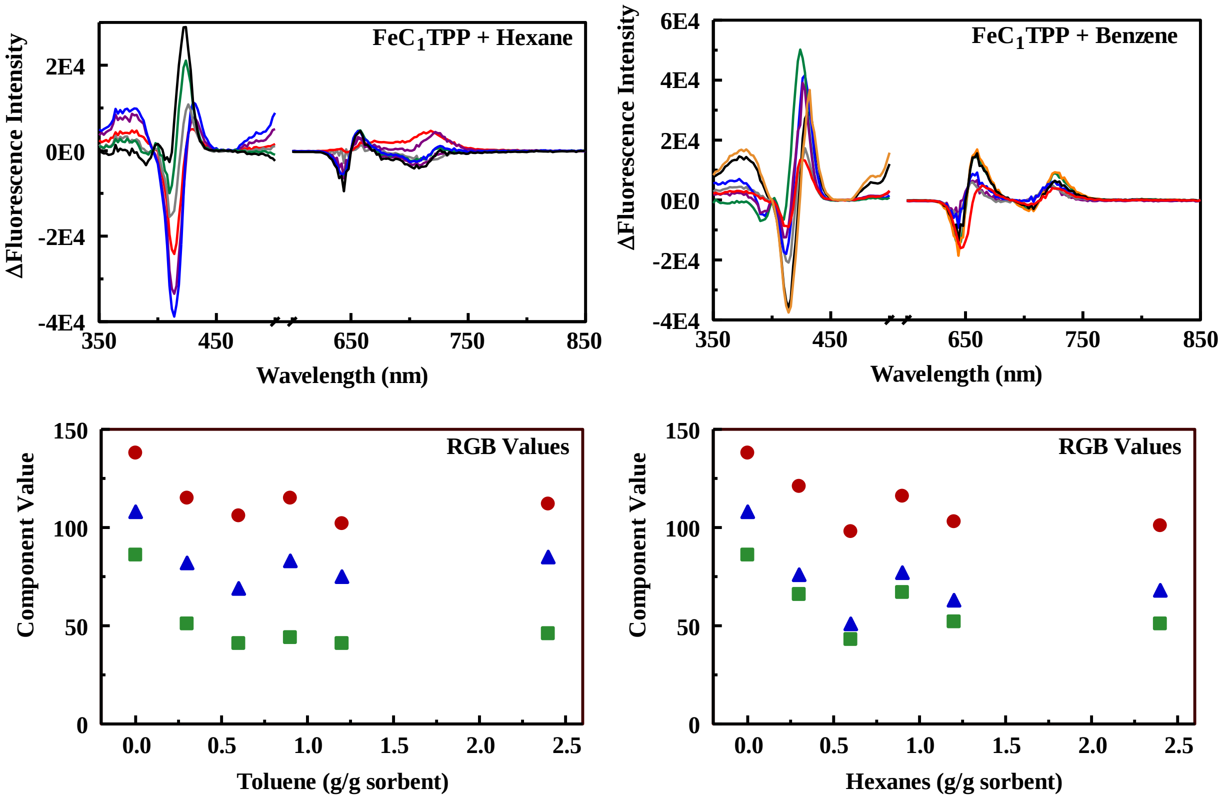

Figure S5. Interaction of C_1TPP-embedded B100 with targets. Shown here are the changes in fluorescence characteristics, simulated images generated based on average RGB values, and the dependence of RGB image color values on target concentration for the interaction of targets with C_1TPP-embedded B100. Changes in fluorescence intensity versus concentration are based on peak/trough differences generated by peak fitting the excitation difference spectra.

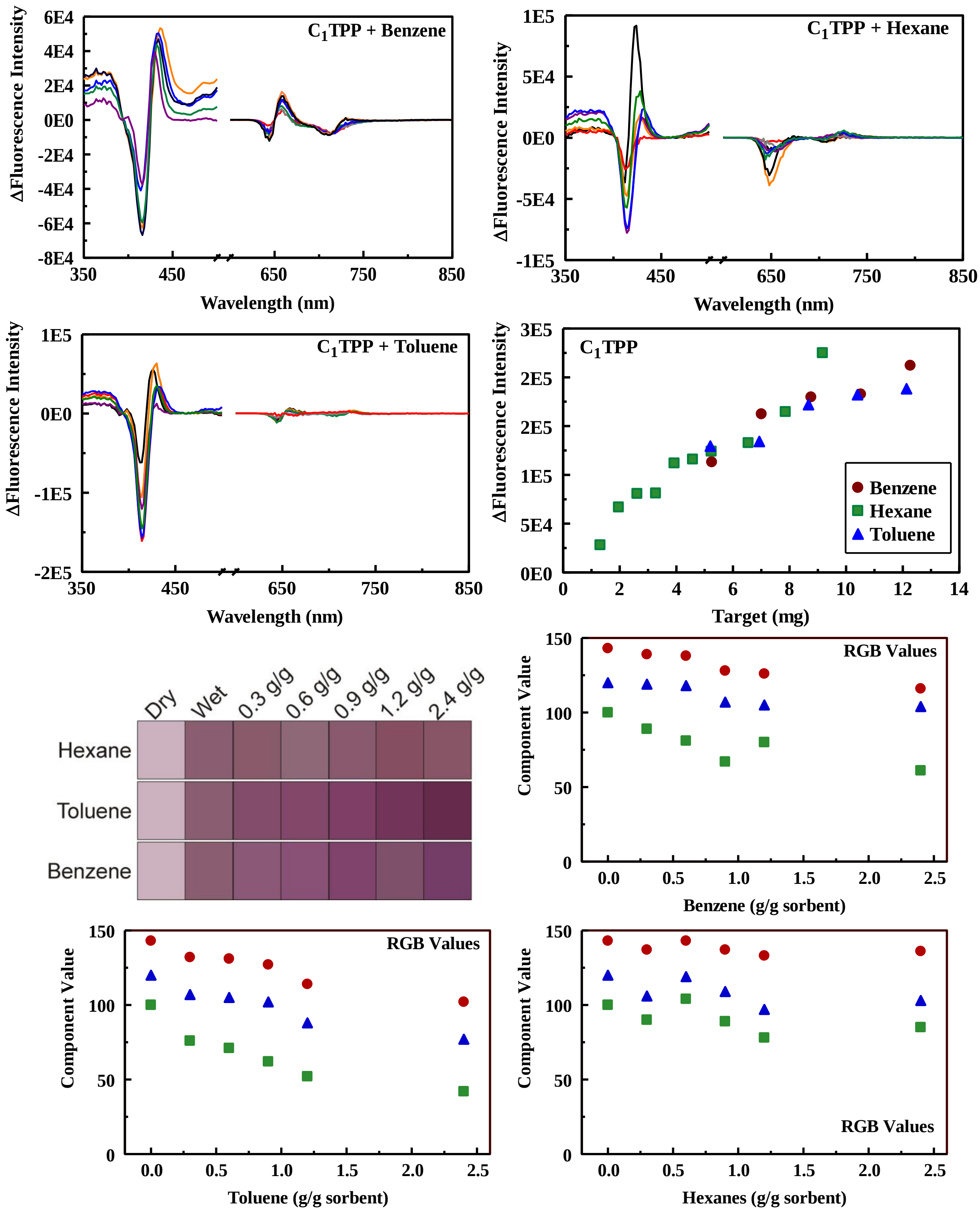

Figure S6. Interaction of MnC_1TPP-embedded B100 with targets. Shown here are the changes in fluorescence characteristics, simulated images generated based on average RGB values, and the dependence of RGB image color values on target concentration for the interaction of targets with MnC_1TPP-embedded B100. Changes in fluorescence intensity versus concentration are based on peak/trough differences generated by peak fitting the excitation difference spectra.

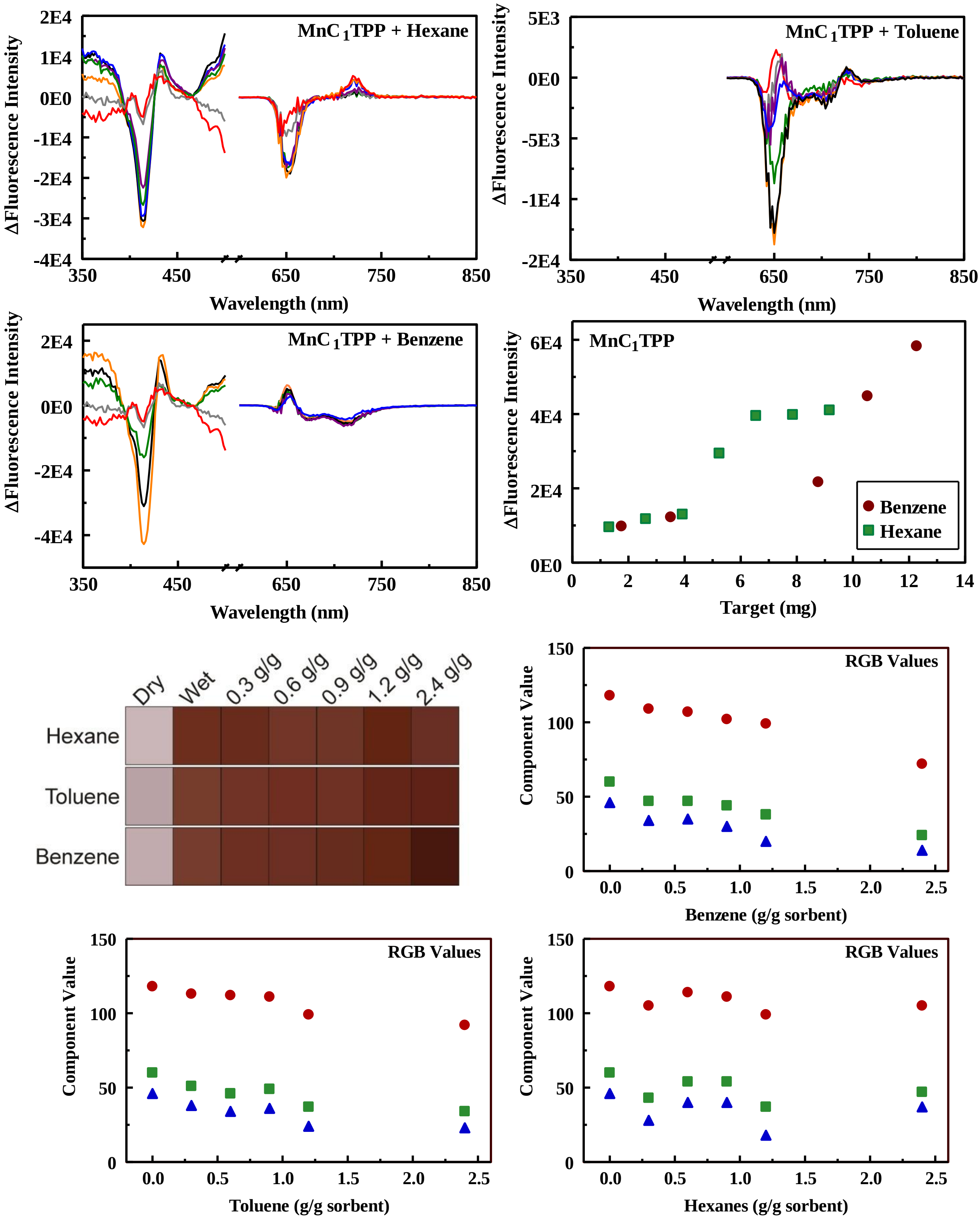

Figure S7. Interaction of C_4TPP-embedded B100 with targets. Shown here are the changes in fluorescence characteristics, simulated images generated based on average RGB values, and the dependence of RGB image color values on target concentration for the interaction of targets with C_4TPP-embedded B100. Changes in fluorescence intensity versus concentration are based on peak/trough differences generated based on the emission difference spectra.

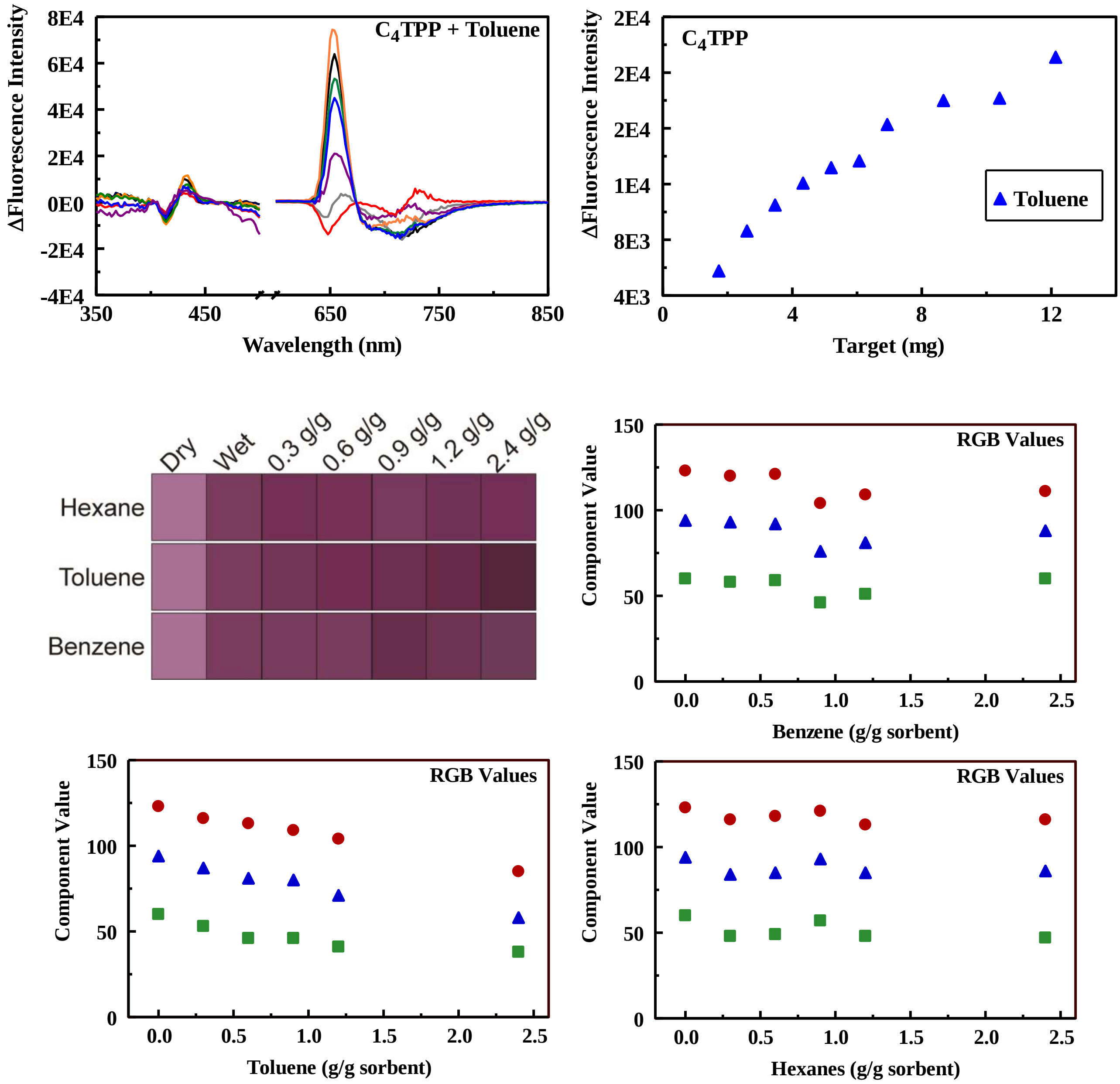

Figure S8. Interaction of FeC_4TPP-embedded B100 with targets. Shown here are the changes in fluorescence characteristics, simulated images generated based on average RGB values, and the dependence of RGB image color values on target concentration for the interaction of targets with FeC_4TPP-embedded B100. Changes in fluorescence intensity versus concentration are based on peak/trough differences from emission difference spectra.

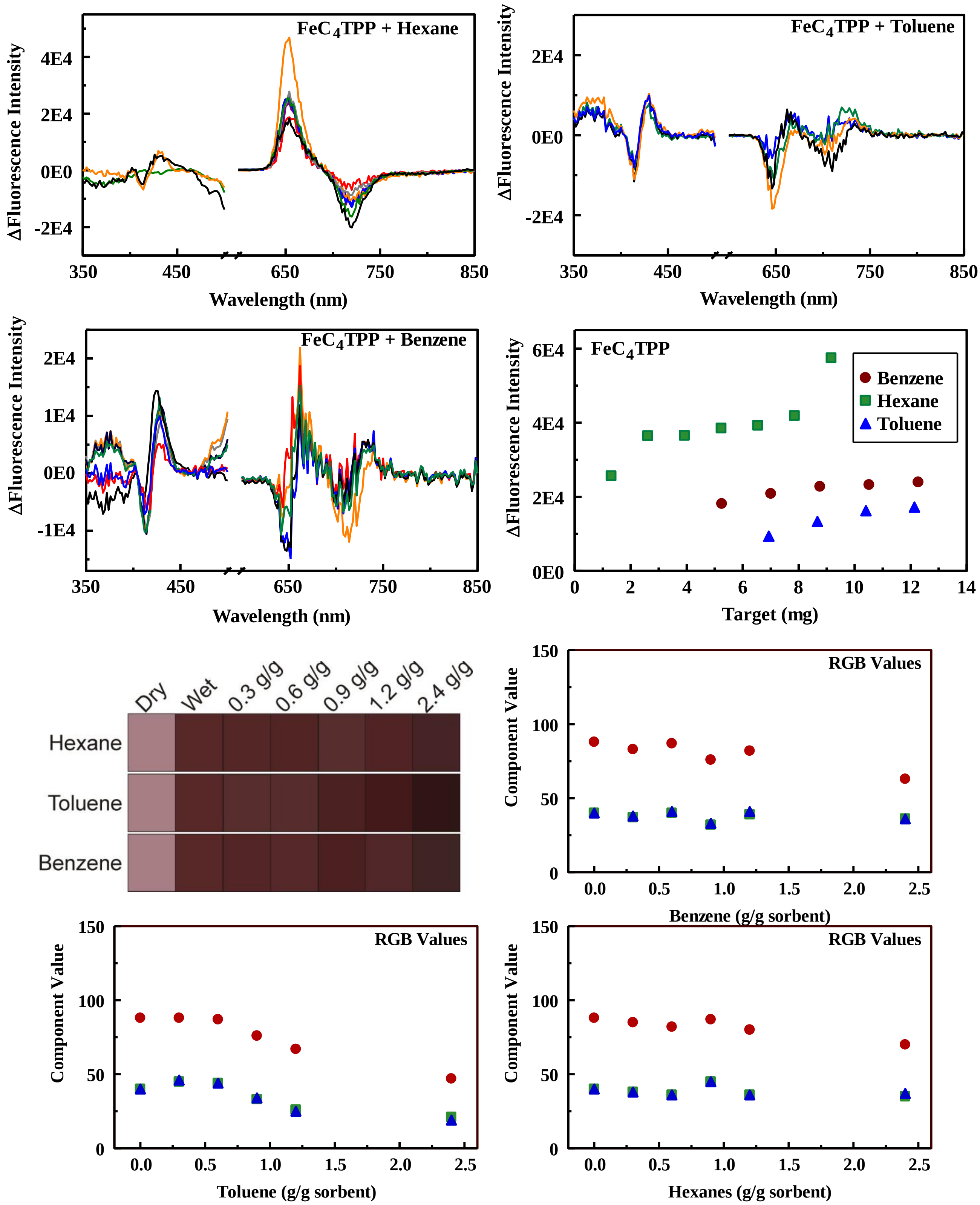

Figure S9. Interaction of MnC_4TPP-embedded B100 with targets. Shown here are simulated images generated based on average RGB values for FeC_1TPP-embedded B100 following exposure to varying target concentrations and the dependence of RGB image color values on target concentration for the interaction of the targets with MnC_4TPP-embedded B100. No changes in fluorescence were observed upon exposure of MnC_4TPP-embedded B100 to the targets.

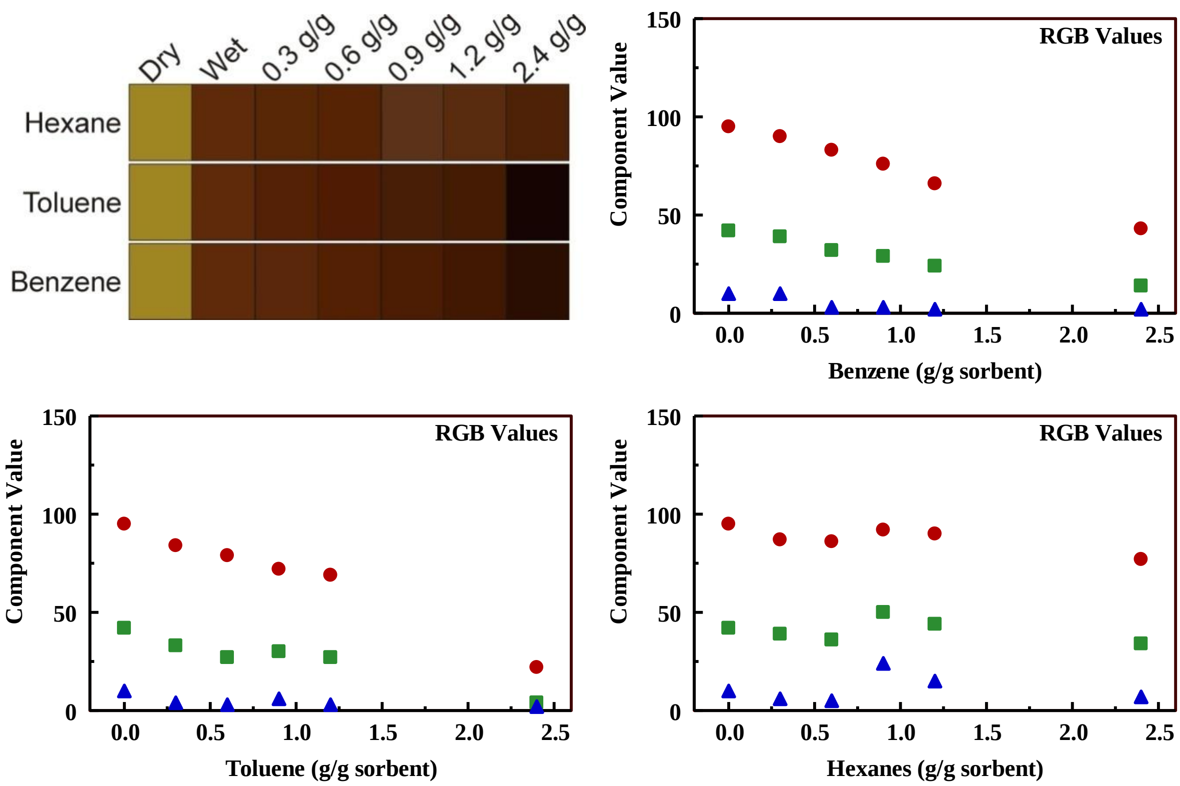

Figure S10. Reflectance spectra. Spectra for the seven different colors used for conversion from RGB to reflectance values. For the reason of solution convergence, the algorithm ignores scaling issues when converting from spectra to RGB leading to some reflectance values greater than 1. A penalty factor is added to the cost function whenever any value of the spectrum exceeds 1.

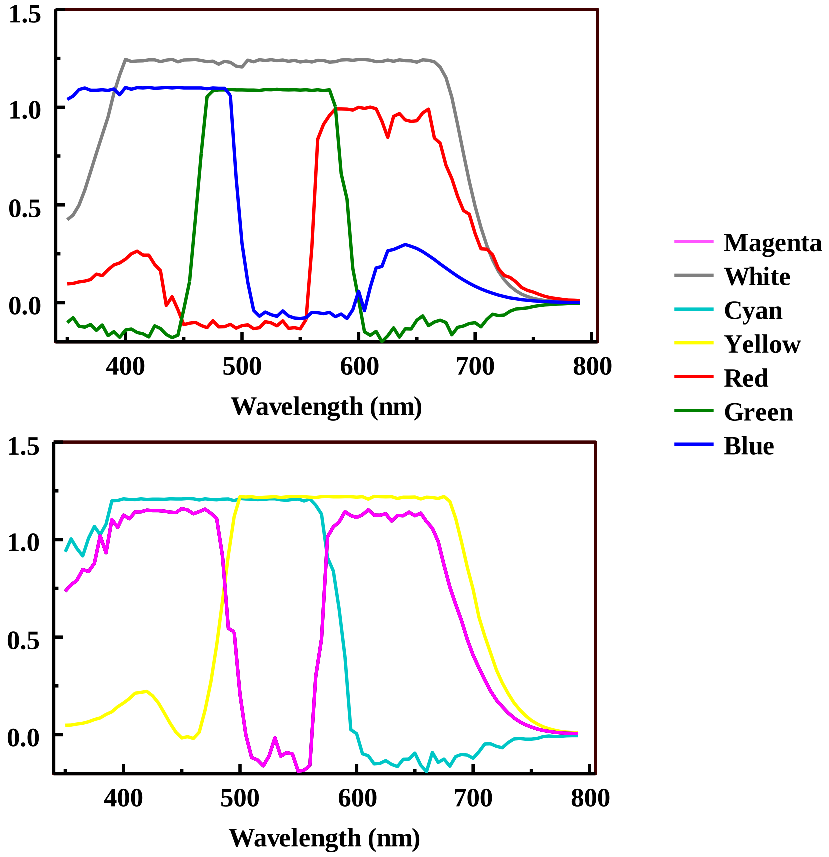

Figure S11. Simulated spectra for interaction of C_1TPP-embedded B100 (5 mg) with the targets. Shown here are reflectance spectra generated based on RGB values (Figure S5) using the color spectra from Figure S10.

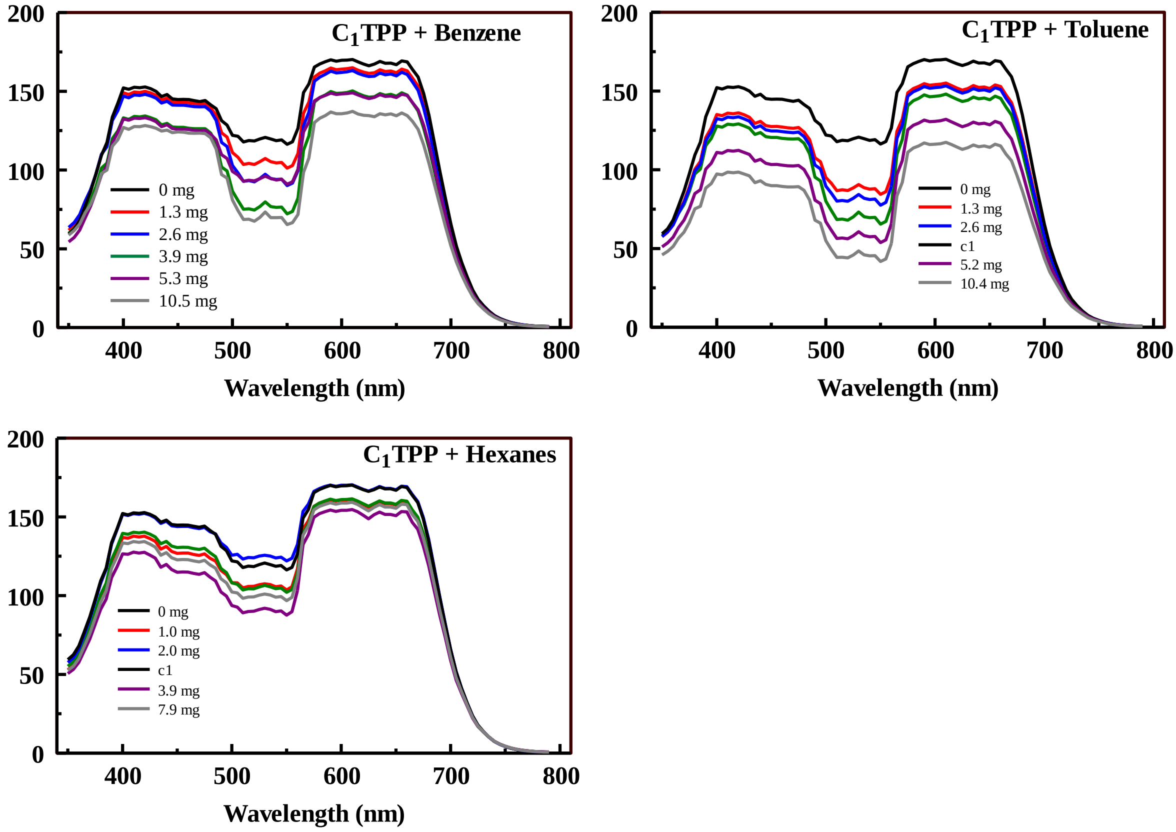

Figure S12. Simulated spectra for interaction of FeC_1TPP-embedded B100 (5 mg) with the targets. Shown here are reflectance spectra generated based on RGB values (Figure S4) using the color spectra from Figure S10.

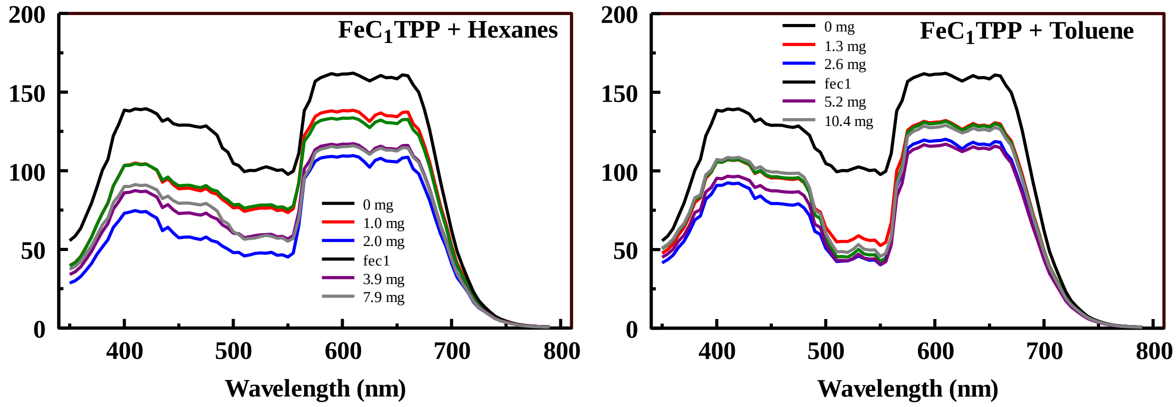

Figure S13. Simulated spectra for interaction of MnC_1TPP-embedded B100 (5 mg) with the targets. Shown here are reflectance spectra generated based on RGB values (Figure S6) using the color spectra from Figure S10.

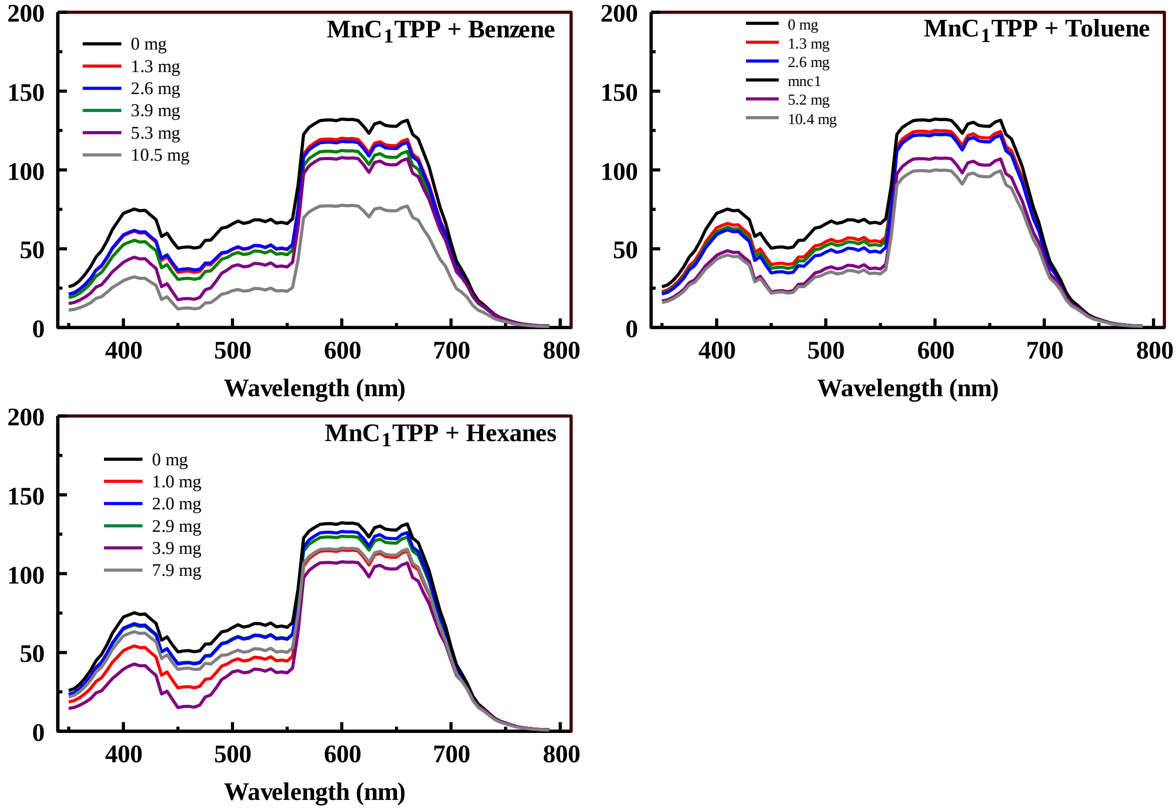

Figure S14. Simulated spectra for interaction of C_4TPP-embedded B100 (5 mg) with the targets. Shown here are reflectance spectra generated based on RGB values (Figure S7) using the color spectra from Figure S10.

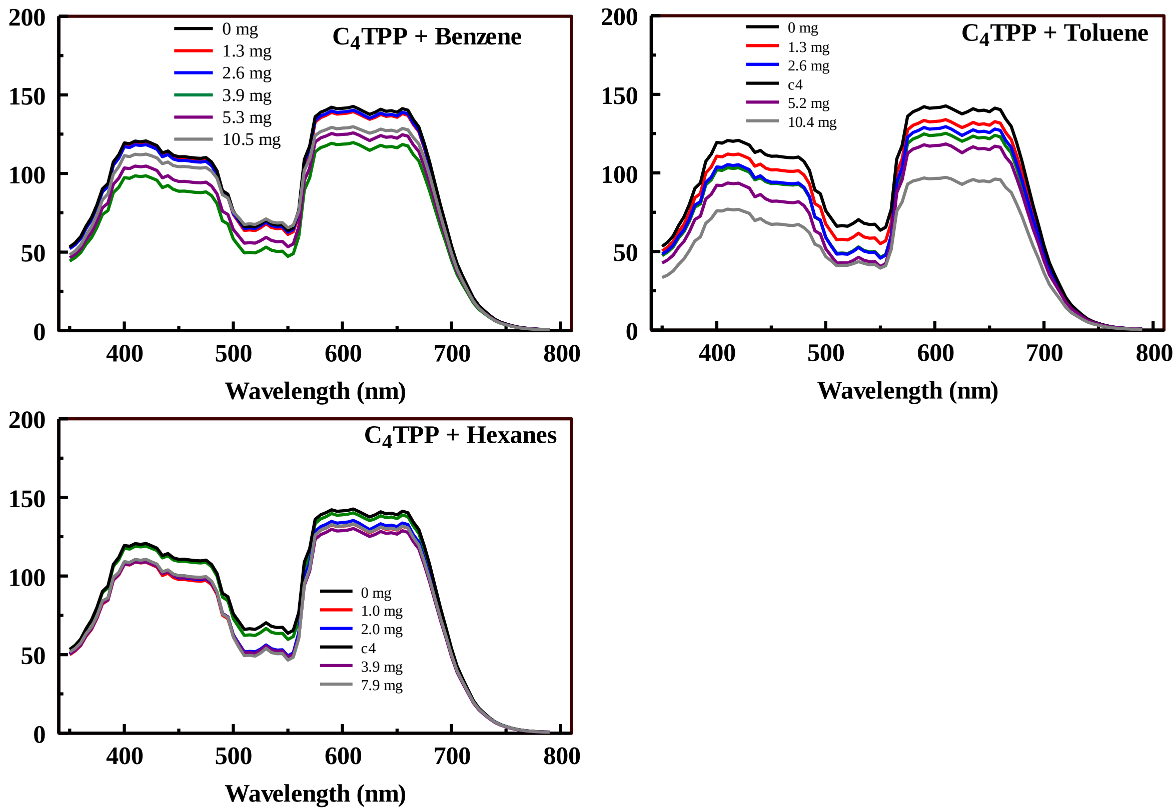

Figure S15. Simulated spectra for interaction of FeC_4TPP-embedded B100 (5 mg) with the targets. Shown here are reflectance spectra generated based on RGB values (Figure S8) using the color spectra from Figure S10.

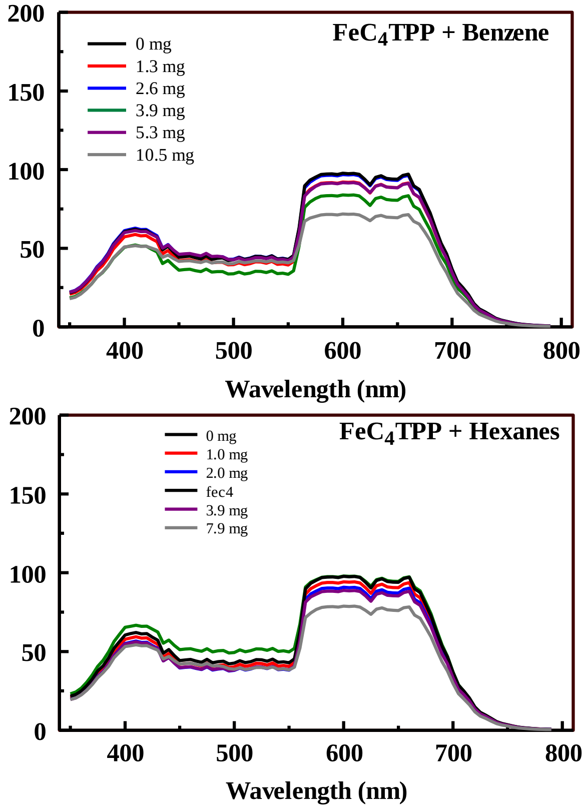

Figure S16. Simulated spectra for interaction of MnC_4TPP-embedded B100 (5 mg) with the targets. Shown here are reflectance spectra generated based on RGB values (Figure S9) using the color spectra from Figure S10.